Effects of Digitization and JPEG Compression on Land Cover Classification Using Astronaut-acquired Orbital Photographs

Ensuring high quality digital data transfer for an increasingly popular imagery type

Edward L. Webb[1] (email: ewebb@ait.ac.th) (author for correspondence)

Julie A. Robinson[2]

Ma. Arlene Evangelista[1,3]

[1]School of Environment, Resources and Development
Asian Institute of Technology
P.O. Box 4 Klong Luang
Pathumthani 12120
Thailand

[2]Office of Earth Sciences
NASA – Johnson Space Center
Lockheed Martin Space Operations
2400 NASA Road 1, C23
Houston, TX 77058-3799
U.S.A.

[3]Current address:
Basic Co., Ltd.
East Tower 5F 16-11 Sakae-Cho
Takasaki City, Gunma 370
Japan

ABSTRACT

Studies that utilize astronaut-acquired orbital photographs for visual or digital classification require high-quality data to ensure accuracy. The majority of images available must be digitized from film and electronically transferred to scientific users. This study examined the effect of scanning spatial resolution (1200, 2400 pixels per inch [21.2 and 10.6 μm/pixel]), scanning density range option (Auto, Full) and compression ratio (non-lossy [TIFF], and lossy JPEG 10:1, 46:1, 83:1) on digital classification results of an orbital photograph from the NASA – Johnson Space Center archive. Qualitative results suggested that 1200 ppi was acceptable for visual interpretive uses for major land cover types. Moreover, Auto scanning density range was superior to Full density range. Quantitative assessment of the processing steps indicated that, while 2400 ppi scanning spatial resolution resulted in more classified polygons as well as a substantially greater proportion of polygons < 0.2 ha, overall agreement between 1200 ppi and 2400 ppi was quite high. JPEG compression up to approximately 46:1 also did not appear to have a major impact on quantitative classification characteristics. We conclude that both 1200 and 2400 ppi scanning resolutions are acceptable options for this level of land cover classification, as well as a compression ratio at or below approximately 46:1. Auto range density should always be used during scanning because it acquires more of the information from the film. The particular combination of scanning spatial resolution and compression level will require a case-by-case decision and will depend upon memory capabilities, analytical objectives and the spatial properties of the objects in the image.

Keywords: archiving, data transfer, image classification, image processing, NASA, remote sensing, scanning, Space Shuttle

INTRODUCTION

The use of astronaut photographs – hand-held photographs of earth taken by astronauts in orbit – for visual interpretation of earth-based processes is well established (Walsh, 1989, Wood, 1989, Helfert et al., 1990, Andrae, 1993, Robbins *et al.*, 1997, Wilkinson *et al.*, 1998, Eckart *et al.*, 1999, Evans *et al.*, 1999, Glasser *et al.*, 1999, Nedeltchev, 1999, Robinson *et al, 1999*, Wilkinson *et al.*1999, Webb *et al.* in press). Because the NASA archive of orbital photographs is historical (images since the 1960's), massive (approaching 400,000 images) and public domain (http://eol.jsc.nasa.gov), it is particularly interesting to explore possible widespread applications using digitized photographs.

Recently, it was reported that high quality astronaut photographs show excellent performance for land use classification (Webb *et al.* in press). The ability to use astronaut photographs for digital classification in addition to visual analysis strengthens the ability of the photographs to complement other satellite imagery. However, digital interpretation of astronaut photographs requires consistently high quality data from the source. It is therefore a primary concern to ensure that the quality of astronaut photographic data remains high from the moment of image capture to eventual digital classification. Such concerns include (among others) camera and lens type, film protection and storage, developing, photographic duplication, and practicalities of image archiving and transfer. The details of the imaging system (including a discussion of cameras, lenses, and films) and spatial resolution are discussed by Robinson *et al.* (in preparation). This paper addresses two important post-capture, pre-analysis processing steps that affect the degree to which information in the film is transferred to the digital format: digitization and compression.

The digitizing process, when the 55mm x 55mm image is digitally scanned, is performed by off-the-shelf hardware with software offering hundreds of variable settings. Although such

software provides a maximum of user flexibility, it has not provided simple ways to standardize the digitizing process. Two important decisions arise during digitization. First is scanning spatial resolution. Photo geometries and frame size determine the area on the ground represented in a photograph. The digitizing spatial resolution then determines the size of the area represented by each pixel in the image (Robinson *et al.*, in preparation). However, the digitizing spatial resolution must also be considered relative to the spatial resolving power of the film. The decision involves determining which digitizing spatial resolution would result in the optimal combination of maximum information transmission and minimum file size. The second decision to make during scanning is to set the density range (the difference in density between the lightest and darkest tones in the image). For example, the density range can be set so that the scanner automatically calculates the optimum density range by measuring the density values of the brightest and darkest areas.

As digital technology has improved, NASA has implemented high-resolution batch digitizing of all Earth photography from recent missions[1]. It is likely that as desktop digitizing hardware becomes more common, scientists will digitize from film products acquired from NASA vendors and use those images in remote sensing analyses. Therefore, it is important to assess the potential effects of basic scanning options on image quality.

File compression is used to improve FTP transfer times of astronaut photographs. Images can be archived and transferred as TIFFs with LZW (non-lossy) compression. To save disk space and speed FTP transfer, particularly outside North America, images may also be compressed using the JPEG algorithm. JPEG is a lossy compression method that results in loss of some color information, while retaining brightness. The effect of JPEG compression on a digital image was

[1] High resolution digitization of Earth observation photographs from older missions will be undertaken in the future. In the interim, single images of older missions are being digitized on a case-by-case basis and supplied to the public.

investigated by Lammi & Sarjakoski (1995), who found that a compression ratio of up to 10:1 did not greatly alter image quality. However, whether JPEG compression of an orbital photograph affects classification results has not been addressed.

We were concerned that manipulation of an image through the processing steps above might introduce errors into digitized version of photograph data, which in turn could affect digital classification results. It is of great interest to evaluate the influence of scanning and archiving options on image quality, because these features are associated with file size, and can indicate the optimal combinations of processing factors that will minimize file size while maximizing information retention. This information can also help NASA to best serve the scientific community when it provides digital images of Earth to the public.

The purpose of this study was to examine differences in visual analysis and digital classification of an orbital photograph as a function of the following image manipulation options:

- Film scanning spatial resolution (1200 v. 2400 pixels per inch, ppi)
- Density range during scanning (Automatic v. Full in PhotoLook™)
- Compression algorithm and level (TIFF v. three JPEG levels)

The use of orbital photographs is already relatively widespread and gaining in popularity, thus the results of this study have relevance to a broad scientific audience.

METHODS

For this investigation we used the orbital photograph STS059-100-058, a near-vertical image of the Chanthaburi coastline, eastern Thailand (Figure 1). The image was captured on 15 April 1994 by the crew aboard Space Shuttle Endeavour, using a Hassleblad camera equipped with a 250 mm

lens and Kodak Aerochrome 2443 thin base CIR film. The altitude of the Shuttle at acquisition was 215 km, and the image exhibited high spatial resolution that allowed accurate digital classification (Webb *et al.* in press). The archived image was located via the Johnson Space Center World Wide Web site (http://eol.jsc.nasa.gov) and high-resolution digitizing was done by special request at the Office of Earth Sciences, Johnson Space Center.

The photographic frame was scanned into digital format via an Agfa Arcus II™ scanner using PhotoLook™ 3.03 software. This scanner has a maximum optical spatial resolution of 2400 x 1200ppi, with 2400 ppi interpolated in the vertical direction. For this study, the image was scanned at both 1200 ppi and at 2400 ppi. Four ***image types*** (Table 1) resulted from the four combinations of scanning spatial resolution and density range control options, hereafter referred to as 1200 Auto, 1200 Full, 2400 Auto, and 2400 Full.

The digital images were saved under various archiving options available in Photoshop™ 4.0 (Table 1). For each image type, we saved the file in TIFF (no compression) and three JPEG compression levels as available in Photoshop™: Level 10 ('low compression' ratio of approximately 10:1), Level 5 ('moderate compression' ratio of approximately 46:1), and Level 1 ('high compression' ratio of approximately 83:1). Photoshop™ software does not allow the user to specify the compression ratio, rather only a qualitative degree of compression from 1 to 10. The final compression ratio achieved will vary depending on the contents of the image, and on the specific JPEG algorithm used for compression. The compression ratio for this study was obtained by comparing the file sizes between the uncompressed TIFF file and the JPEG-compressed file of the image. A total of 16 combinations were evaluated during this study (2 spatial resolutions x 2 density ranges x 4 compression levels; Table 1).

A 159 km^2 portion (12.6 km x 12.6 km based on the geocorrected image) was selected for classification, and clipped from each image type (hereafter, sub-image; Figure 1). The rationale

for using a sub-image was to save both time and disk space during analysis. The sub-image provided a representative array of land use classes exhibited in a moderately complex spatial pattern. Classification of sub-images using the 3 color channels as bands (RGB) was accomplished using ERDAS Imagine™ v8.2. Because a geocorrected form of the entire photograph was classified for another study (Webb *et al.* in press), we had available training sites and were able to add to the existing array in the sub-image using visual interpretation, existing land use maps, and our field experience in the study region.

Classification of each sub-image used a maximum likelihood algorithm that resulted in eight terrestrial and sea categories (Webb *et al.* in press): mangroves, Veg1 (low vegetation such as grasslands and highly degraded former mangrove habitat), Veg2 (vegetation intermediate in density and height), Veg3 (dense tropical forest and tree plantations, e.g. rubber, durian, etc.), sea, sediment, bare soil, and aquaculture (shrimp ponds abundant in the area [Delsol & Ly, 1994]).

Analysis of the classified image was undertaken on two spatial scales. First, the sub-image was used to compare overall classification consistency among image types. Second, a portion of that sub-image, hereafter referred to as the 'sub-image detail', was selected for quantitative examination of the differences in polygon attributes across the 16 scanning x compression options (Figure 1). As above, choosing the sub-image detail conserved disk space and analysis time. This area of 12,321 pixels (111 pixels x 111 pixels) digitized at 2400 ppi, corresponded to 1.17 mm x 1.17 mm on the original film, and approximately 1.2 km x 1.2 km on the ground.

RESULTS

Qualitative assessment of sub-image detail

Auto v. Full density range options (TIFF images). We visually assessed the differences in classification between Auto and Full option TIFF images. Comparing only TIFF images controlled for possible effects of JPEG compression on visual interpretation. Visual assessment between Auto and Full options revealed that for both 1200 and 2400 ppi scanning spatial resolution, Auto options exhibited less apparent stochastic image degradation (i.e., small groups of apparently misclassified pixels) and a smoother classified image (Figure 2). This is demonstrated in the bottom right quadrants of the classified TIFF images, where the polygons in the Full option images exhibit a low vegetation (yellow) border between mid vegetation and bare soil. Moreover, the Full option appeared to increase the level of noise, manifested by higher heterogeneity within polygons, particularly in the 2400 ppi image. An example of this can be seen as speckling in the left half of all 2400 Full images. The increased noise in the Full option image is generally consistent across both 1200 and 2400 JPEG compression options, supporting the interpretation that the border and noise effects were the result of the Full option rather than scanning spatial resolution or compression options. Therefore, we concluded that the Automatic density range is preferable to Full density range option for capturing meaningful information from the film. We then concentrated the rest of the visual analyses on the Auto option images only; however quantitative analysis did include Full option images.

1200 ppi v. 2400 ppi (TIFF Auto images). Not surprisingly, the greatest visual difference resulting from scanning spatial resolutions was the smoothness of the polygon boundaries (Figure 2). Visually, the classifications using the 1200 ppi and 2400 ppi TIFF Auto images performed similarly, despite differences in pixel size. The greatest difference between the two resolutions

can be found in the top left quadrant, where the 2400 ppi image classified sediment, and the 1200 ppi image identified aquaculture with mangroves (Figure 2). In general, however, major polygons are similar in size and shape between the two resolutions. Overall, the classification differences between 1200 and 2400 ppi scanning appear to be very minor and visually the classification arising from the two spatial resolutions were largely in agreement.

Effect of JPEG compression (Auto images). The JPEG compression resulted in only minor effects on the image classification, most evident in the 83:1 compression image (Figure 3). Possible degradation events due to 83:1 compression can be seen in the top left quadrant of the 2400 ppi images (note the mangroves near the top of the image) and the bottom left quadrant (the Sea polygon – obviously a misclassification but nevertheless somewhat degraded). The 46:1 compression was visually in high agreement with the TIFF image, indicating that this moderate compression generated results that are probably acceptable for any visual application.

Quantitative analysis of the sub-image detail

The effect of scanning spatial resolution, density range, and compression on classification was quantitatively assessed using two methods. First, we compared differences in the total area devoted to each classification category. Second, the size-class distributions of land use polygons were compared across classified images.

Effect of JPEG compression on overall sub-image classification

There was a high consistency in the percent of pixels in each classification category across all compression levels (Table 2). Quantitative assessment of the variability across JPEG compressions was achieved by examining the coefficient of variation (CV, expressed as %) for

each class. The highest variability was in the 1200 Auto image, which exhibited the highest average CV at 2.88; lowest variability was at 2400 Auto (Table 2). Overall the very low CV values indicate that compression did not vary substantially across levels for each image type.

To evaluate which image type had the highest consistency between JPEG and TIFF, we first calculated the mean percentage for each class across JPEG options within each image type. Then the deviate for each JPEG and TIFF class was calculated as $|\text{TIFF} - \text{mean JPEG}|$ (Table 2). The overall consistency between JPEG and TIFF for an image type was calculated as the sum of square roots (SSR) of all class deviates: $\sqrt{(|\text{TIFF} - \text{mean JPEG}|)}$. Sum of square roots was used rather than sum of squares (Sokal and Rohlf, 1981) because all deviates were <1.0. The SSR was smallest for the 2400 Auto image (SSR = 2.71, Table 2). These results indicate that the highest level of agreement between JPEG and TIFF in terms of proportional allocation of the image to similar classes was in the 2400 Auto. Thus, the 2400 Auto image type had the highest consistency in final classification among JPEG compression levels, and also the highest consistency with TIFF. Interestingly, the 46:1 compression ratio resulted in the lowest mean deviation from the TIFF classification for three of the four image types (Table 2, Figure 4). This indicates that JPEG compression of up to 46:1 was not detrimental to the classification results of this image.

Effect of scanning spatial resolution, density range and compression on sub-image detail polygon attributes

We compared effects of scanning spatial resolution, density range and compression on classified polygon attributes across the four types of sub-image details. Polygons were grouped according to size (i.e. area); size classes were made comparable across spatial resolutions by adjusting size class ranges to adjust for pixel dimensions. For example, the smallest polygon size class for the

1200 ppi image was 1-5 pixels, and for the 2400 ppi image 1-19 pixels. Based on a pixel size of approximately 10m for the 2400 ppi image (Webb *et al.* in press), approximate polygon size classes were <0.2 ha, 0.2-0.4 ha, 0.4-0.8 ha, 0.8-1.2 ha, etc.

Scanning spatial resolution affected the classification results in two ways (Table 3). First, the total number of polygons in the 2400 ppi images was greater than their corresponding images at 1200 ppi. This was expected based on the higher number of total pixels. Second, the proportion of polygons in the smallest size class (<0.2 ha) was greater in the 2400 ppi images than their corresponding images at 1200 ppi. Comparing the size class distribution between 1200 Auto TIFF and 2400 Auto TIFF (Table 3, Figure 5) reveals that the proportion of polygons in the smallest size class is >20% greater in the 2400 ppi Auto TIFF images than in the corresponding 1200 ppi image, with similar results for JPEG (Table 3). This result was consistent for the Full option images, with the 2400 ppi image exhibiting substantially more polygons in the smallest size class for both TIFF and JPEG.

The effect of scanning density range (Auto v. Full) on polygon attributes was evaluated by comparing the TIFF polygon size class distributions between Auto and Full images (Figure 5). The influence of density range is particularly evident in the small polygon size class, where the Full options had a substantially greater proportion of polygons in that size class. This agrees with the visual interpretation suggesting greater levels of internal heterogeneity and perhaps noise in the Full option image.

The number of polygons created in the TIFF classification was compared with the JPEG values for that image using the point-to-distribution comparison described by Sokal and Rohlf (1981). In all cases, the number of polygons in the TIFF image was not different than the distribution created by the three JPEG options, indicating that there was consistency in polygon

size classification between the TIFF image and JPEG compressed images (for all tests, $df = 2$, $t_{critical} = 4.303$; $t_{1200Auto} = 2.13$, $t_{1200Full} = 2.82$, $t_{2400Auto} = 2.07$, $t_{2400Full} = 3.73$).

DISCUSSION

Visual comparison of Auto versus Full density range options indicated that the Full option tended to increase stochastic noise in the image, characterized by errors around the border of many polygons, combined with increased heterogeneity within polygons. This result suggests that the Auto option is preferable to the Full option, and any astronaut photograph to be visually or digitally analyzed should be digitized in this manner. To transfer this result to other equipment and software, the important consideration is to ensure that the density spread of the digitizer does not cut off information either at the low or high end of the intensity range. In other words, settings should be selected so that subtle differences in the film intensity very near to black and very near to white are preserved.

The relationship between image spatial resolution – whether based on a scanning sensor or scanning resolution used to digitize film – and spatial autocorrelation (i.e. the probability that an adjacent pixel will have the same value) is a complex phenomenon (Woodcock & Strahler, 1987). The spatial structure of an image will in part dictate the maximum spatial resolution attained at minimum cost (memory). Thus, the optimal spatial resolution at which one can digitally analyze an astronaut photograph will also depend upon spatial structure, which will vary across images. Although determining the optimal spatial resolution for analysis of a satellite image is a complex task, astronaut photographs pose even more difficulty because of the numerous platform-specific factors bearing on the ultimate spatial structure of the image, including shuttle altitude, lens focal length, look angle, and light conditions (Robinson *et al.* in preparation).

Astronaut photographs can vary greatly in spatial resolution qualities, and the image used for this study exhibited high resolution for an astronaut photograph (each pixel ca. 10 m at 2400 ppi). The high image quality resulted from the combination of a low Shuttle altitude (215 km), long lens focal length (250 mm), near vertical look angle, high spatial and spectral contrast in land use reflectances, and near cloud-free conditions (Webb *et al.* in press). It is interesting to note that there was a high level of agreement between overall classifications of the 1200 ppi and 2400 ppi TIFF images (Table 2). This is despite the fact that 2400 ppi had a substantially greater percentage of polygons in the smallest size class (Table 3). Because this astronaut photograph exhibited very high quality for its altitude and focal length, small pixels can be expected to hold useable spatial information. Nevertheless, our analysis indicated that even with the possible minor loss of spatial information, classification was not compromised. In this instance a 1200 ppi scanning spatial resolution would not affect data integrity.

For many other astronaut photographs, spatial distortion due to oblique look angle will increase the variability in spatial scale across the image. In oblique photographs the spatial scale nearer to the nadir position is much finer than the spatial scale away from the nadir of the spacecraft (see Robinson *et al*, in preparation). For oblique photographs that are going to be georeferenced, an image may need to be digitized at the maximum spatial resolution justifiable by the film resolving power in order to obtain the maximum spatial information away from the nadir position.

Many astronaut photographs with potential for remote-sensing applications have less-optimal photographic conditions (e.g., sun elevation angle, exposure, film type) than the image used in this study. For these lower quality images the amount of basic information available in the film is reduced, and there may be little relative advantage of higher digitizing spatial resolution. Therefore, whether the possible increase in spatial resolution that 2400 ppi offers justifies a file

2.5 times larger (for JPEG) or 4 times larger (for TIFF) than a 1200 ppi image (Table 1) is a decision that needs to be made for each image, and depends upon image spatial resolution, other elements of image quality, land use complexity, and spatial scale of the objects of interest.

We recommend the following method for determining the appropriate digitizing spatial resolution for a land use study using an astronaut photograph. First, estimate the expected diameters of relevant land use polygons that will be classified. Then estimate the distance on the ground covered across the center of the photograph as recommended by Robinson *et al.* (in preparation). This gives a sense of the area on the ground that will be represented by pixels at different digitizing spatial resolutions. Select a digitizing resolution that will provide multiple pixels for each relevant polygon without exceeding the resolving power of the film. Our rule of thumb for polygons is a minimum width of 5 pixels per polygon.

As an example we apply this method to the image used in this study, which exhibited fewer than 10 land use/cover classifications. Suppose we were interested in classifying polygons of 100 m or greater in diameter. The original 55 mm x 55 mm image is 49.3 km across at its center point. Thus the minimum diameter of a polygon of interest would be approximately 1/493 of the image, i.e.111 μm on the original film. Applying the 5 pixel rule, the film digitized at 1200 ppi (21.2 μm/pixel) would result in an image in which 5 pixels represent 106 μm on the original film, less than the required 111 μm. Thus, digitizing at 1200 ppi (10.6 μm/pixel) would be sufficient for these objectives. The results in this paper provide support for this method of digitization.

Given a certain disk space allocation, which alternative is better: a 1200 ppi image with low compression, or a 2400 ppi image with higher compression? For example, if one were to analyze the image used in this study, but wanted to limit file size to 5Mb, the best image alternatives would be 1200 ppi / 10:1 compression, or 2400 ppi / 46:1 compression for Auto

density images (Table 1). Overall classifications between the two images would be expected to be similar (see Table 2), however there would be discrepancies in polygon size class distributions as described earlier (Table 3). Therefore, the appropriate scanning spatial resolution and compression level will depend on the spatial scale and shapes of polygons that are of interest.

Our results suggest that JPEG compression of astronaut-acquired orbital photographs results in no appreciable visible image degradation, and is an acceptable algorithm for the archiving and transfer of image data for many purposes. Overall classification results were consistent across JPEG compression levels, and were consistent with classification results of a TIFF archived image. Moreover, there was little variation in polygon attributes among JPEG compression levels, or between JPEG and TIFF. Researchers obtaining images in JPEG compressed format should therefore feel confident that data integrity for visual analysis and general classifications is high, particularly if compression levels remain below a compression ratio of less than approximately 46:1.

The influence of JPEG compression on spurious introduced error in an image classification may vary according to the size of polygons and the uniformity of reflectance within the polygons. It has been observed that the JPEG compression algorithm will introduce error into large polygons of homogeneous data (R. Schumann, personal communication). Therefore, our results should be considered an initial investigation, and it would be useful to investigate whether spurious errors introduced by JPEG influences classification, and how this is related to polygon size and heterogeneity.

ACKNOWLEDGEMENTS

To be entered later as per instructions.

REFERENCES

Andrae, M. O., 1993, Global distribution of fires seen from space. EOS, Transactions of the American Geophysical Union 74: 129, 135.

Delsol, J.P., and Ly, Li., 1994, The use of multi-temporal remote sensing data for evaluating the impact of shrimp culture on the coastal zone in Chantaburi Province, Thailand. Unpublished report, Asian Institute of Technology.

Eckardt F.D., Wilkinson J., and Lulla, K.P., 1999, Terrain visualization using digitized Shuttle photography and global DEM. International Journal of Remote Sensing (in press).

Evans, C. A. Robinson, J.A., Runco, S., Wilkinson, M.J., Dickerson, P.W., Amsbury, D.L., and Lulla, K.P., 1999, The 1997-1998 El Niño: Images of floods and drought taken from the Mir. In Lulla, K.P. and L. Dessinov, eds, Global changes: new observations from Mir (in press).

Glasser, M., Lulla, K.P., and Wilkinson, M.J., 1999, Surveying biomass burning and smoke palls from NASA-Mir missions (1996-1998). In Lulla, K.P. and L. Dessinov, eds, Global changes: new observations from Mir (in press).

Helfert, M. R., Mohler, R. R. J., and Giardino, J. R. , 1990, Measurement of areal fluctuations of Great Salt Lake, Utah, using rectified space photography. Houston Geological Society Bulletin 32: 16-19.

Lammi, J., and Sarjakoski, T., 1995, Image compression by the JPEG algorithm. Photogrammetric Engineering and Remote Sensing 61: 1261-1266.

Nedeltchev, N.M., 1999, Space Shuttle Photography - a powerful tool of remote sensing investigation of human effects on earth. International Journal of Remote Sensing 20: 183-188.

Robbins, L.L., Tao, Y., and Evans, C.A., 1997, Temporal and spatial distribution of whitings on Great Bahama Bank and a new lime budget. Geology 25: 947-950.

Robinson, J.A., McRay, B., and Lulla, K.P., 1999, Twenty-eight years of urban growth in North America quantified by analysis of photographs from Apollo, Skylab and NASA-Mir. In Lulla, K.P. and L. Dessinov, eds, Global changes: new observations from Mir (in press).

Walsh, C.H., 1989, Meteorological applications of space shuttle photography. Geocarto International 4: 39-48.

Webb, E.L., Evangelista, M.A., and Robinson, J.A. (in press), Digital land use classification using Space Shuttle-acquired orbital photographs: a quantitative comparison with Landsat TM imagery of a coastal environment, Chanthaburi, Thailand. Photogrammetric Engineering and Remote Sensing.

Wilkinson, M.J., White, L.G., and Lulla, K.P., 1998, Evolution of rural ghettoes in northeastern South Africa as viewed from the Space Shuttle. Geocarto International (in press).

Wilkinson, M.J., Wheeler, J.D., Charlson, R.J., and Lulla, K.P., 1999, Imaging aerosols from low-earth orbit: photographic results from the NASA/MIR and Shuttle Programs. In Lulla, K.P. and L. Dessinov, eds, Global changes: new observations from Mir.

Wood, C.A., 1989, Geologic applications of space shuttle photography. Geocarto International 4: 49-54.

Table 1. Matrix of image types (spatial resolutions x density range) and compression options used to archive the orbital photograph in this study. File sizes (megabytes) are in parentheses.

	Scanning Spatial Resolution	
Density range	1200 ppi	2400 ppi
Auto	TIFF (18.6)	TIFF (74.2)
	JPEG 83:1 (0.38)	JPEG 83:1 (0.96)
	JPEG 46:1 (0.64)	JPEG 46:1 (1.7)
	JPEG 10:1 (3.1)	JPEG 10:1 (7.9)
Full	TIFF (18.6)	TIFF (74.3)
	JPEG 83:1 (0.32)	JPEG 83:1 (0.83)
	JPEG 46:1 (0.58)	JPEG 46:1 (1.5)
	JPEG 10:1 (2.8)	JPEG 10:1 (7.3)

Table 2. Results of classification of the four sub-image types (1200 Auto, 1200 Full, 2400 Auto, 2400 Full). Compression refers to TIFF (no compression) or JPEG ratio (see text). Numbers under Compression columns indicate the percent of the image classified in that category.

1200 AUTO	Compression							
Class Name	TIFF	10:1	46:1	83:1	Mean JPEG	CV (%)	Deviate |TIFF-JPEG|	Sqrt Dev
Sea	27.1	26.8	26.8	26.6	26.7	0.29	0.36	0.60
Sediment	15.3	13.9	15.4	15.1	14.8	5.38	0.50	0.71
Mangrove	5.0	5.0	5.2	5.7	5.3	6.76	0.32	0.57
Aquaculture	21.6	22.7	20.9	20.5	21.4	5.48	0.17	0.41
Low Vegetation	10.9	11.2	11.3	11.3	11.3	0.80	0.31	0.56
Mid Vegetation	6.9	7.0	7.0	7.1	7.1	0.84	0.14	0.37
High Vegetation	1.9	1.9	2.0	2.0	2.0	2.74	0.07	0.26
Bare soil	11.3	11.5	11.4	11.6	11.5	0.77	0.19	0.44
Mean Dev from TIFF		0.43	0.25	0.44				
Mean CV (%)						2.88		
Sum of Square Roots								3.91

1200 FULL	Compression							
Class Name	TIFF	10:1	46:1	83:1	Mean JPEG	CV (%)	Deviate |TIFF-JPEG|	Sqrt Dev
Sea	28.2	27.8	27.8	27.6	27.7	0.54	0.43	0.66
Sediment	14.6	15.4	15.1	15.0	15.2	1.16	0.61	0.78
Mangrove	6.3	6.2	6.3	6.8	6.4	4.90	0.10	0.32

Aquaculture	22.0	21.8	22.0	21.7	21.9	0.75	0.19	0.43
Low Vegetation	9.4	9.1	9.1	9.0	9.1	0.56	0.29	0.54
Mid Vegetation	7.2	7.3	7.3	7.5	7.3	1.55	0.19	0.43
High Vegetation	2.0	2.0	2.0	2.0	2.0	0.21	0.01	0.12
Bare soil	10.3	10.3	10.3	10.4	10.3	0.39	0.01	0.10
Mean Dev from TIFF		0.24	0.16	0.33				
Mean CV (%)						1.26		
Sum of Square Roots								3.38

2400 AUTO

	Compression						
Class Name	TIFF	10:1	46:1	83:1	Mean JPEG	CV (%)	Deviate |TIFF-JPEG|	Sqrt Dev
Sea	24.5	24.8	24.8	24.6	24.7	0.56	0.25	0.50
Sediment	17.0	17.0	17.1	17.2	17.1	0.52	0.11	0.33
Mangrove	5.9	5.8	5.7	5.8	5.8	0.56	0.08	0.28
Aquaculture	21.1	21.0	21.0	20.8	20.9	0.58	0.20	0.45
Low Vegetation	9.2	9.0	9.0	9.1	9.0	0.47	0.13	0.36
Mid Vegetation	8.9	8.7	8.7	8.8	8.8	0.60	0.11	0.33
High Vegetation	2.0	2.0	2.0	2.0	2.0	0.31	0.00	0.05
Bare soil	11.6	11.7	11.7	11.8	11.7	0.62	0.17	0.41
Mean Dev from TIFF		0.13	0.15	0.14				
Mean CV (%)						0.53		
Sum of Square Roots								2.71

2400 FULL	Compression							
Class Name	TIFF	10:1	46:1	83:1	Mean JPEG	CV (%)	Deviate |TIFF-JPEG|	Sqrt Dev
Sea	23.18	23.82	23.72	23.73	23.76	0.25	0.57	0.76
Sediment	19.71	19.16	19.44	19.61	19.40	1.18	0.30	0.55
Mangrove	4.55	4.59	4.55	4.76	4.63	2.47	0.08	0.29
Aquaculture	24.29	24.55	24.49	24.17	24.40	0.83	0.12	0.34
Low Vegetation	9.26	9.06	9.01	8.63	8.90	2.66	0.35	0.60
Mid Vegetation	7.26	6.92	6.89	7.09	6.97	1.59	0.30	0.54
High Vegetation	1.92	2.04	2.04	1.93	2.01	3.12	0.09	0.29
Bare soil	9.84	9.86	9.87	10.07	9.93	1.18	0.09	0.30
Mean Dev from TIFF		0.27	0.22	0.25				
Mean CV (%)						1.66		
Sum of Square Roots								3.68

Table 3. Polygon size class distributions for TIFF and three JPEG compression options for each sub-image detail of the four image types.

1200 Auto

					JPEG Compression Level					
			TIFF		10:1		46:1		83:1	
Size Class	Pixels	Approximate Area (ha)	Freq.	%	Freq.	%	Freq.	%	Freq.	%
1	1-4	< 0.20	59	35.33	58	35.15	38	26.21	61	39.61
2	5-9	0.20 – 0.36	31	18.56	36	21.82	33	22.76	23	14.94
3	10-19	0.40 – 0.76	22	13.17	19	11.52	23	15.86	18	11.69
4	20-29	0.80 – 1.16	11	6.59	13	7.88	7	4.83	9	5.84
5	30-39	1.20 – 1.56	8	4.79	7	4.24	7	4.83	4	2.60
6	40-59	1.60 – 2.36	8	4.79	6	3.64	10	6.90	7	4.55
7	60-99	2.40 – 3.96	5	2.99	5	3.03	5	3.45	12	7.79
8	100-199	4.00 – 7.96	9	5.39	8	4.85	8	5.52	8	5.19
9	200-499	8.00 – 19.96	7	4.19	4	2.42	5	3.45	6	3.90
10	> 500	≥ 20.00	7	4.19	9	5.45	9	6.21	6	3.90
TOTAL			167		165		145		154	

1200 Full

					JPEG Compression Level					
			TIFF		10:1		46:1		83:1	
Size Class	Pixels	Approximate Area (ha)	Freq.	%	Freq.	%	Freq.	%	Freq.	%
1	1-4	< 0.20	166	57.44	191	61.41	204	63.95	214	59.94
2	5-9	0.20 – 0.36	39	13.49	46	14.79	35	10.97	48	13.45
3	10-19	0.40 – 0.76	28	9.69	18	5.79	28	8.78	27	7.56

4	20-29	0.80 – 1.16	15	5.19	10	3.22	6	1.88	12	3.36
5	30-39	1.20 – 1.56	6	2.08	10	3.22	7	2.19	15	4.20
6	40-59	1.60 – 2.36	8	2.77	7	2.25	9	2.82	13	3.64
7	60-99	2.40 – 3.96	6	2.08	8	2.57	7	2.19	6	1.68
8	100-199	4.00 – 7.96	4	1.38	6	1.93	6	1.88	9	2.52
9	200-499	8.00 – 19.96	10	3.46	9	2.89	11	3.45	7	1.96
10	> 500	20.00	7	2.42	6	1.93	6	1.88	6	1.68
TOTAL			289		311		319		357	

2400 Auto

			JPEG Compression Level							
			TIFF		10:1		46:1		83:1	
Size Class	Pixels	Approximate Area (ha)	Freq.	%	Freq.	%	Freq.	%	Freq.	%
1	1-19	< 0.20	144	56.69	159	60.92	191	65.86	213	65.74
2	20-39	0.20 – 0.39	34	13.39	23	8.81	24	8.28	26	8.02
3	40-79	0.40 – 0.79	17	6.69	28	10.73	17	5.86	30	9.26
4	80-119	0.80 – 1.19	9	3.54	6	2.30	12	4.14	9	2.78
5	120-159	1.20 – 1.59	12	4.72	13	4.98	9	3.10	9	2.78
6	160-239	1.60 – 2.39	9	3.54	6	2.30	7	2.41	9	2.78
7	240-399	2.40 – 3.99	11	4.33	7	2.68	11	3.79	8	2.47
8	400-799	4.00 – 7.99	4	1.57	5	1.92	4	1.38	6	1.85
9	800-1999	8.00 – 19.99	7	2.76	7	2.68	8	2.76	7	2.16
10	> 2000	20.00	7	2.76	7	2.68	7	2.41	7	2.16
TOTAL			254		261		290		324	

2400 Full

			JPEG Compression Level							
			TIFF		83:1		46:1		10:1	
Size Class	Pixels	Approximate Area (ha)	Freq.	%	Freq.	%	Freq.	%	Freq.	%
1	1-19	< 0.20	270	72.97	329	78.33	338	78.60	285	72.89
2	20-39	0.20 – 0.39	26	7.03	26	6.19	24	5.58	40	10.23
3	40-79	0.40 – 0.79	19	5.14	19	4.52	14	3.26	21	5.37
4	80-119	0.80 – 1.19	10	2.70	4	0.95	10	2.33	7	1.79
5	120-159	1.20 – 1.59	14	3.78	5	1.19	8	1.86	5	1.28
6	160-239	1.60 – 2.39	7	1.89	11	2.62	12	2.79	7	1.79
7	240-399	2.40 – 3.99	3	0.81	5	1.19	4	0.93	3	0.77
8	400-799	4.00 – 7.99	6	1.62	7	1.67	6	1.40	10	2.56
9	800-1999	8.00 – 19.99	9	2.43	8	1.90	8	1.86	6	1.53
10	> 2000	20.00	6	1.62	6	1.43	6	1.40	7	1.79
TOTAL			370		420		430		391	

FIGURE LEGENDS

Figure 1. Sub-image of Space Shuttle orbital photograph STS059-100-58 (left) and the sub-image detail (right). No scale bar is represented here because this image was not geocorrected; however from another paper (Webb *et al.*, in press) the approximate spatial resolution of the image is 10 m/pixel.

Fig.2. Land cover classifications of a sub-image detail of NASA photo STS059-100-058, across scanning resolutions and archiving options.

Fig.3. Land cover classifications of a sub-image detail of NASA photo STS059-100-058 across scanning resolutions and compression options.

Figure 4. Mean deviation of polygon classifica tions for JPEG compression from corresponding TIFF classifications for each image type (data from Table 2).

Figure 5. Polygon size class distributions for the classified sub-image detail, scanned at 1200 ppi (top) and 2400 ppi (bottom), Auto or Full density range and archived using the TIFF algorithm.

Figure 1.

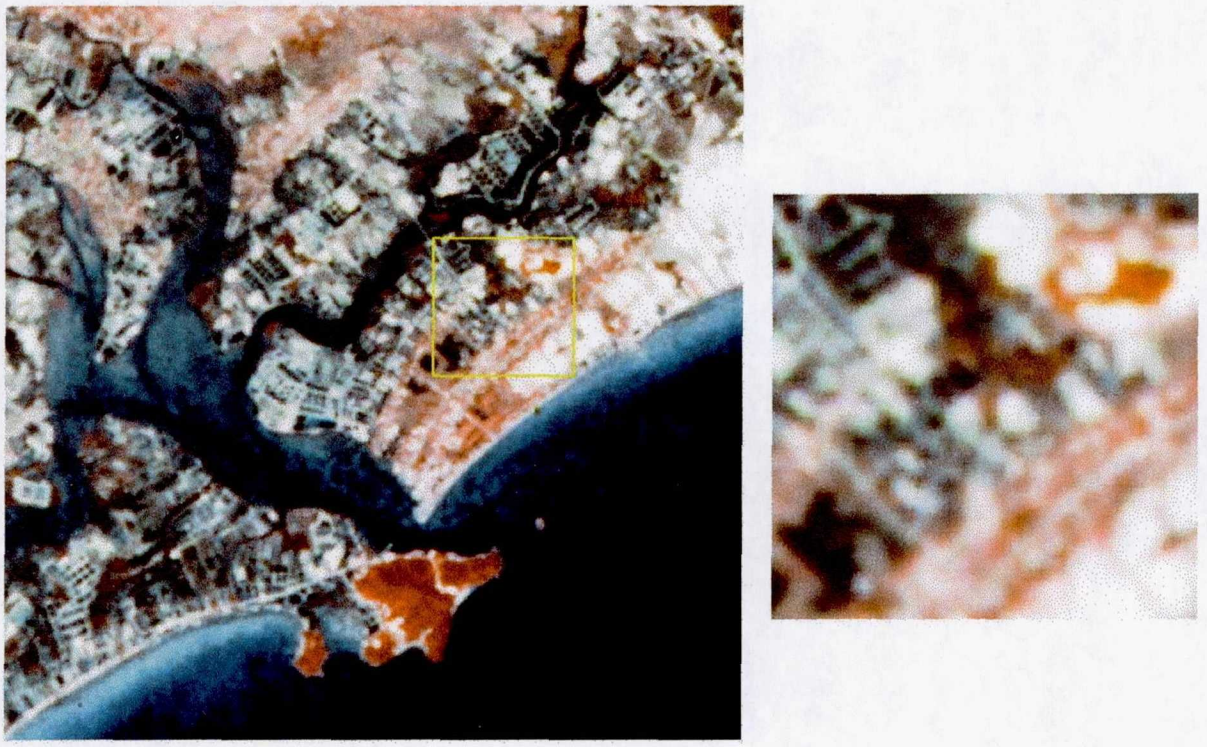

Figure 2.

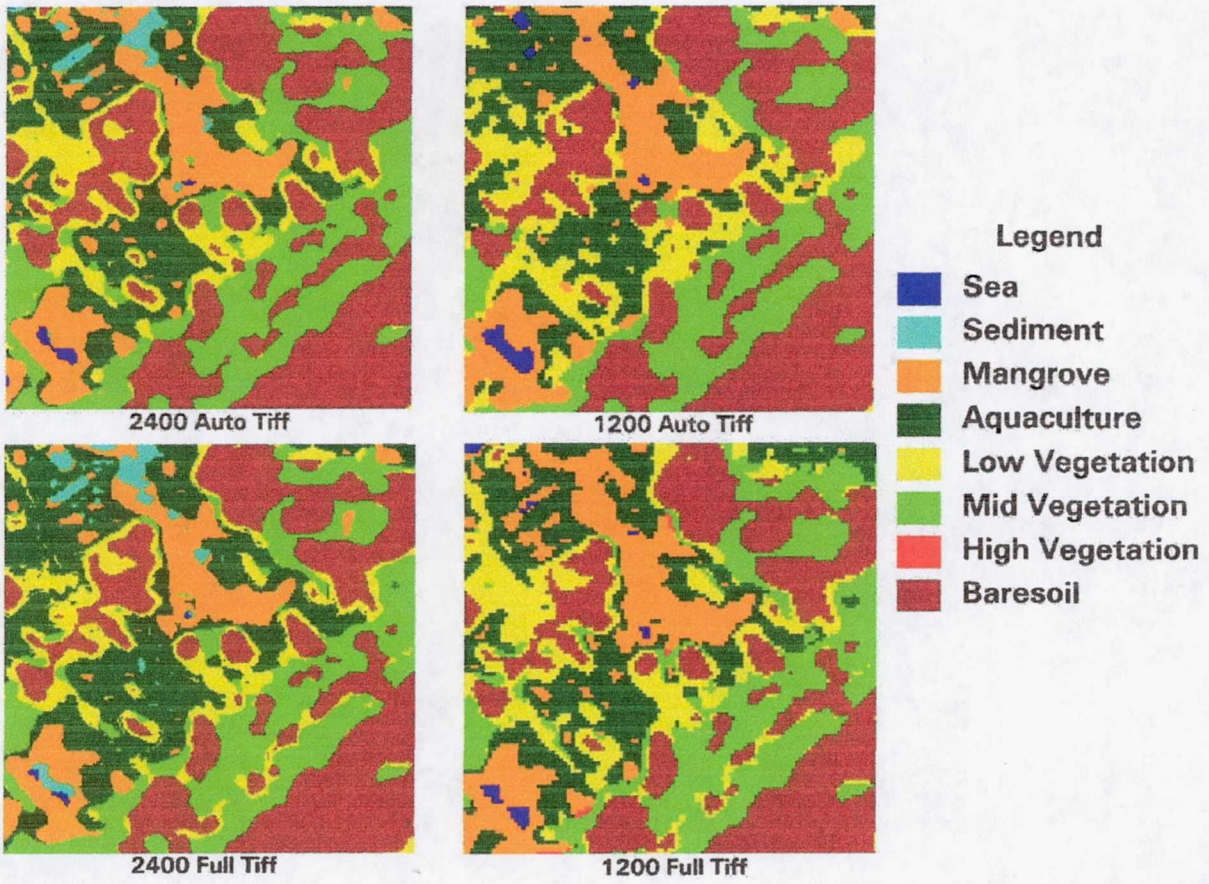
2400 Auto Tiff
1200 Auto Tiff
2400 Full Tiff
1200 Full Tiff
Legend
Sea
Sediment
Mangrove
Aquaculture
Low Vegetation
Mid Vegetation
High Vegetation
Baresoil

Figure 3.

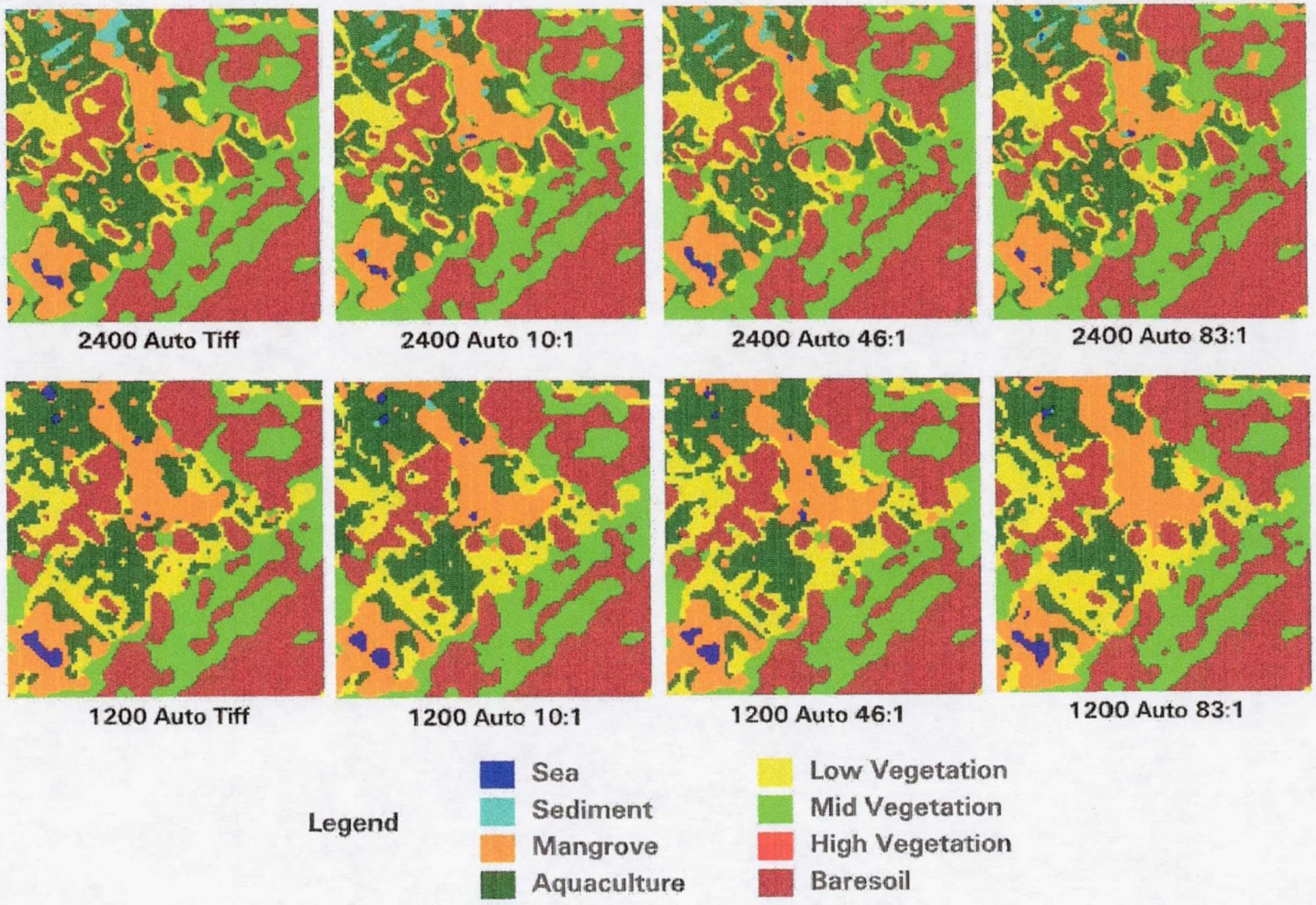
2400 Auto Tiff
2400 Auto 10:1
2400 Auto 46:1
2400 Auto 83:1
1200 Auto Tiff
1200 Auto 10:1
1200 Auto 46:1
1200 Auto 83:1
Legend
Sea
Sediment
Mangrove
Aquaculture
Low Vegetation
Mid Vegetation
High Vegetation
Baresoil